

Self-Healing Performance of Heavyweight Concrete with Steam Curing

Hideki Igawa, Yoshinori Kitsutaka, Takashi Yokomuro, Hideo Eguchi

Abstract—In this study, the crack self-healing performance of the heavyweight concrete used in the walls of containers and structures designed to shield radioactive materials was investigated. A steam curing temperature that preserves self-healing properties and demolding strength was identified. The presented simultaneously mixing method using the expanding material and the fly ash in the process of admixture can maximize the self-curing performance. Also adding synthetic fibers in the heavyweight concrete improved the self-healing performance.

Keywords—Expanding material, heavyweight concrete, self-healing performance, synthetic fiber.

I. INTRODUCTION

RESEARCH and development is currently underway on the use of heavyweight concrete for containers to store various debris, including contaminated construction waste materials from radiation leakage accidents [1], [2]. Due to the outstanding capacity of heavyweight concrete to shield against radiation, this work is also examining the potential use in structural walls. To date, use of heavyweight concrete in Japan has been limited to a narrow range of applications, including use as ballast weights on cargo ships and as shielding walls at nuclear power stations. Relative little research has been done on using heavyweight concrete for storage containers or wall materials or on the durability of heavyweight concrete in such applications. The water tightness of concrete is a key factor in applications that involve shielding against radiation. After curing, concrete in particular poses the risk of cracking when subject to external stresses, including paste contraction on drying and temperature-related volume fluctuations. Water ingress via cracks can generate water leaks and corrode steel reinforcement, ultimately degrading structural durability. While cracks in concrete are typically repaired by injecting chemical solutions, a concrete used for radioactive shielding applications should be maintenance-free. We studied the self-healing properties of concrete capable of self-repair. Various past studies have examined admixtures of fly ash and expanding materials, as well as the use of granulation technology [3]-[6]. Hydrating unreacted cement particles promotes self-healing, but the effects are believed to be

H. Igawa and H. Eguchi are with the Technical Research Institute, Nippon Hume Corp., Kumagaya, Japan (e-mail: h-igawa@nipponhume.co.jp, h-eguchi@nipponhume.co.jp).

Y. Kitsutaka is with the Faculty of Urban Environmental Sciences, Tokyo Metropolitan University, Tokyo, Japan (phone: #81-42-677-2797; fax: #81-42-677-2797; e-mail: kitsu@tmu.ac.jp).

T. Yokomuro is with the Department of Innovative Engineering Architecture Course, Ashikaga Institute of Technology, Tochigi, Japan (e-mail: yokomuro@ashitech.ac.jp).

relatively modest for concrete subjected to steam curing or other accelerated curing. There has been little research using steam curing. However, circumstances associated with radioactive contamination generally require rapid construction, making use of pre-cast concrete an effective course of action. In such cases, steam curing is essential to produce heavyweight concrete.

In this study, we investigated the self-healing performance of steam-cured heavyweight concrete, examining the range of steam temperatures that preserved self-healing qualities, and seeking to identify the types and amounts of synthetic fibers suited to self-healing.

II. OUTLINE OF EXPERIMENT

A. Used Materials

Table I lists the materials used in this study. Table II lists the properties of the synthetic fibers used. The cement used was ordinary Portland cement. The fine and coarse aggregate used consisted of a mixture of dust containing a high proportion of iron and metal slag, fused as heavyweight aggregate, which was crushed and graded appropriately.

TABLE I
PROPERTIES

Materials	Symbol	Properties
Cement	C	Ordinary Portland cement, Density: 3.16 g/cm ³ Specific surface: 3332 cm ² /g
Expansive admixture	EX	Ettringite type, Density: 3.01 g/cm ³
Fly ash	FA	JISII Type, Density: 2.20 g/cm ³ Metal slag aggregate 0-5, Water absorption 1.67%, F.M.3.83
Fine aggregate	S	Metal slag aggregate 20-05, Water absorption 0.7%, F.M.6.52 Saturated surface-dry particle density: 4.20 g/cm ³
Coarse aggregate	G	Saturated surface-dry particle density: 4.29 g/cm ³
Fiber	F1	Polypropylene short fiber Density: 0.91 g/cm ³
	F2	Nylon short fiber Density: 1.16 g/cm ³
	F3	Vinylon short fiber Density: 1.30 g/cm ³
Water	W	Water supply
Chemical admixture	SP1	High-range water-reducing admixture: Polycarboxylate type
Air-entraining agent	SP2	Modified rosin acid compound-based anionic surfactant

A. Test Specimen

We performed permeability tests to evaluate self-healing performance quantitatively. The permeability test specimen was a square column sample 14 days after atmospheric curing, in which simulated cracking was induced at the center section

by a bending test rig. The test specimen was sandwiched between aluminum plates measuring 0.2 mm in thickness to maintain the cracking width, and then clamped using a steel jig and steel rods tightened with a torque wrench to a uniform 40 Nm. The sides sandwiched between the plates were sealed to allow unidirectional water permeation.

TABLE II
 PROPERTIES OF SYNTHETIC FIBERS

Symbol	Density (g/cm ³)	Fiber length (mm)	Fiber diameter (mm)	Aspect ratio	Tensile strength (N/mm ²)	Young modulus (N/mm ²)
F1	0,91	12	0,065	185	530	5000
F2	1,16	12	0,015	800	550	4200
F3	1,3	30	0,660	50	900	23000

B. Permeability Test

We performed crack permeability testing to quantitatively evaluate the extent to which the simulated crack region was filled. Fig. 1 shows the permeability test apparatus, which consists of a flat rubber plate (inner diameter 80 mm, outer diameter 90 mm, thickness 2 mm) placed on top of the tested surface of the test specimen (the side face of the specimen when manufactured), on top of which a PVC pipe is placed. An expanded polystyrene float (diameter 70 mm, thickness 10 mm) was placed inside the PVC pipe and a laser displacement gauge mounted on top of this float. The pipe was filled with water, after which we measured the displacement of the float corresponding to the change in water level due to water permeation with a laser displacement gauge. Testing involved measuring the time taken for the water level inside the PVC pipe to drop 10 mm due to water permeation, which was used to calculate the permeability rate (in cm³/s). This was done three times to obtain a mean value used as the test result. The initial value for the permeability rate was taken after immersing all test specimens for 24 hours in an approximately 80 L water tank maintained at constant conditions (20 ± 2 °C, 60% RH ± 5%) in a thermostatic chamber. Tap water was used in the permeability tests and to immerse the test specimens. We performed evaluations after immersing the specimens for 7 days, 14 days, 21 days, and 28 days.



Fig. 1 Permeability test situation

C. Microscopy Observation

We used a crack scale to measure the crack region of the tested surface for the permeability test, marking cracks 0.15 to 0.2 mm wide for examination. We then examined these cracks

after immersing for 7 days, 14 days, 21 days, and 28 days. Examination involved removing the specimen from the water, drying the crack region with a hair dryer, and checking and recording the extent to which the cracks had been filled with a microscope. (Fig. 2)



Fig. 2 Microscopy

D. Concrete Mixture Proportions

Table III gives the concrete mixture proportion conditions. The targeted concrete density (mass per unit volume when dry) was 3.2 t/m³ or greater. The strength for proportioning not including the admixture was set to 50 N/mm². For the purposes of this study, since previous studies [7] had confirmed high self-healing performance using fly ash together with an expansive admixture, we also mixed fly ash and the expansive admixture with the cement by using fly ash as a substitute for some of the fine aggregate. The synthetic fibers used were polypropylene short fibers (F1), nylon short fibers (F2), and vinylon short fiber (F3), with varying proportions with respect to concrete volume. We established a slump flow of 50±10 cm, as specified for the concrete to ensure kneading of fibers, and added a high-performance water-reducing agent and air content regulating agent to obtain the targeted air content of 4.5 ± 1.5%.

E. Concrete Mixing

Using a forced two-shaft mixer, we mixed the heavyweight concrete in batches of 35 L. We mixed the ingredients for one minute without adding water, and then mixed the ingredients for 90 seconds after adding water. The synthetic fiber was scattered as it was added to keep fiber balls from forming. The flow was adjusted using a high-performance water-reducing agent. We then formed compressive strength test specimens as cylindrical specimens measuring 100 mm in diameter x 200 mm in length. The self-healing performance test specimens were formed by pouring into formworks measuring 100 mm (h) x 100 mm (w) x 400 mm (l).

F. Test Factors

Since the hydration of unreacted cement particles promotes self-healing, steam curing and other accelerated curing methods are believed to reduce effectiveness. We therefore studied steam curing temperatures that satisfied demolding strength requirements and ensured adequate self-healing performance. The concrete used in the tests was mixture (EXFA). Fig. 3 shows the steam curing conditions used.

TABLE III
 MIX PROPORTIONS OF CONCRETE

Mix No.	Slump (cm)	flow (%)	W/C (%)	s/a (%)	Unit amount (kg/m ³)								
					W	C	EX	FA	S	G	SP1	SP2	F1~3
EXFA											9,0	0,180	
0.3F1											8,6	0,180	F1 0.3(vol%)
0.6F1											11,3	0,144	F1 0.6(vol%)
0.3F2	50±10		44,3	144	450	60	160	1071	1370	9,5	0,135	F2 0.3(vol%)	
0.6F2											11,3	0,113	F2 0.6(vol%)
0.3F3											9,9	0,122	F3 0.3(vol%)
0.6F3											9,5	0,135	F3 0.6(vol%)

We also studied how the types and amounts of synthetic fibers affected self-healing performance. The synthetic fibers used were polypropylene short fibers (F1), nylon short fibers (F2), and vinylon short fibers (F3), with varying proportions with respect to concrete volume.

Initial permeability rates vary significantly even for identical crack widths and must be regulated within a fixed range because differences therein affect self-healing performance [7]. This was achieved by adjusting the clamping force acting on both sides of the test specimen using the steel jig and steel rods to regulate the initial permeability rate to $0.25 \pm 0.05 \text{ cm}^3/\text{s}$ and $0.55 \pm 0.05 \text{ cm}^3/\text{s}$.

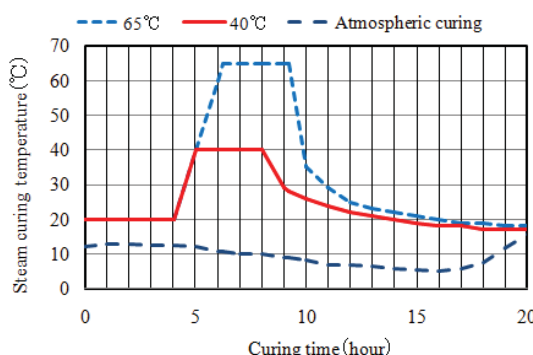


Fig. 3 Curing temperature hysteretic of up to demolding

III. TEST RESULTS

A. Effect of Steam Curing Temperature

Table IV gives the physical properties of the concrete. Fig. 3 shows the curing temperature history from concrete pouring up to demolding. Fig. 4 shows the relationship between the calculated cumulative temperature ($^{\circ}\text{C}\cdot\text{h}$) and compressive strength at demolding. Note that Equation (1) is used to obtain cumulative temperature M.

$$M = \sum_0^t (\theta + A) \Delta t \quad (1)$$

M: Cumulative temperature ($^{\circ}\text{C} \cdot \text{h}$); θ : Temperature of concrete in Δt ($^{\circ}\text{C}$); A: Constant (typically $10 ^{\circ}\text{C}$); Δt : Time

Fig. 4 shows a close correlation between concrete demolding strength and cumulative temperature up to demolding. Pre-cast concrete is generally required to have a demolding strength between 30 and 35 N/mm^2 to ensure it can withstand bending stresses generated by adhesion forces between the formwork

and the concrete and its own weight when lifted. Since these stresses were expected to be even greater in the case of heavyweight concrete, the required demolding strength was set to 40 N/mm^2 . Using 40 N/mm^2 in the regressive formula gave a cumulative temperature of $661 \text{ }^{\circ}\text{C}\cdot\text{h}$. Calculating backward from this cumulative temperature gives a maximum steam curing temperature of $32.5 \text{ }^{\circ}\text{C}$. Since the natural temperature drop after steam curing will be even lower during winter months, we set the maximum steam curing temperature required for demolding to $40 \text{ }^{\circ}\text{C}$.

TABLE IV
 PHYSICAL PROPERTIES OF CONCRETE

Mix No.	Steam curing temperature (°C)	Slump (mm)	Air (%)	Compressive strength (N/mm ²)	
				1d	14d
Atmospheric curing				15,5	56,2
EXFA	40	410×400	3,0	44,7	67,6
	65			56,2	76,4

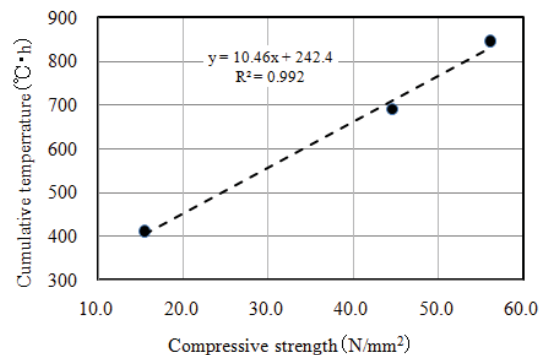


Fig. 4 Demolding strength and cumulative temperature

Fig. 5 shows permeability test results after immersion in water for crack self-healing specimens manufactured under various curing conditions. The permeability rate after immersion for 28 days was lowest for atmospheric curing, then progressively higher for steam curing at $40 \text{ }^{\circ}\text{C}$ and steam curing at $65 \text{ }^{\circ}\text{C}$. This indicates that concrete self-healing performance is particularly affected by initial curing temperature. The maximum steam curing temperature in this test was set to $40 \text{ }^{\circ}\text{C}$ because this meets demolding strength requirements and has minimal effects on self-healing performance. This temperature was also used in subsequent testing.

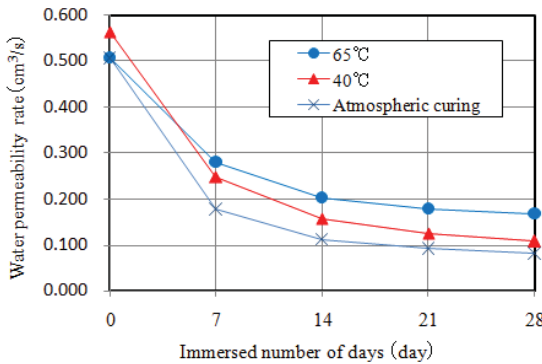


Fig. 5 Permeability test results

B. Effect of Synthetic Fibers

Table V shows the fresh properties and compressive strength of heavyweight concrete intermixed with synthetic fibers. The targeted slump flow was set to 50 ± 10 cm, and the air content was set to $4.5 \pm 1.5\%$.

TABLE V
 TEST RESULTS OF CONCRETE

Concrete Mix No.	temperature (°C)	Slump flow (mm)	Air (%)	Compressive strength (N/mm²)	
				1d	14d
0.3F1	15,9	440×450	5,3	47,3	80,7
0.6F1	17,4	420×400	5,9	33,8	70,0
0.3F2	17,2	520×520	3,6	37,5	80,2
0.6F2	17,5	440×430	3,3	30,1	60,7
0.3F3	18,5	440×440	4,5	45,9	88,1
0.6F3	17,5	410×420	3,6	40,8	84,5

We adjusted the initial permeability rate to 0.25 ± 0.05 cm^3/s and 0.55 ± 0.05 cm^3/s . Fig. 6 shows the results for an initial permeability rate of $0.25 \text{ cm}^3/\text{s}$. Fig. 7 shows the results for an initial permeability rate of $0.55 \text{ cm}^3/\text{s}$. In the two cases, the initial permeability rate was between 0.20 and $0.30 \text{ cm}^3/\text{s}$, and between 0.50 and $0.60 \text{ cm}^3/\text{s}$, respectively. Our tests indicated some self-healing performance for all test specimens. The specimens that showed particularly high self-healing performance and lowest permeability rates after 28 days of immersion were mixture (0.3F3), with an initial permeability rate of $0.25 \text{ cm}^3/\text{s}$, and mixture (0.3F2), with an initial permeability rate of $0.55 \text{ cm}^3/\text{s}$. While higher initial permeability rates tended to correlate with lower self-healing performance, adding synthetic fibers boosted self-healing performance. This may be because self-healing substances tend to adhere to the synthetic fibers and repair cracks [8].

Fig. 8 shows the relationship between synthetic fiber content and permeability rate after 28 days of immersion. Increasing synthetic fiber content did not necessarily increase self-healing performance, which points to a synthetic fiber content that gives optimal self-healing performance. These tests demonstrate the effectiveness of fibers on self-healing, with relative modest differences regardless of type or content. Besides increasing costs, increasing synthetic fiber content reduces workability. We believe that these findings may

suggest the existence pf an ideal content ratio. Further study will be required to determine this ideal amount.

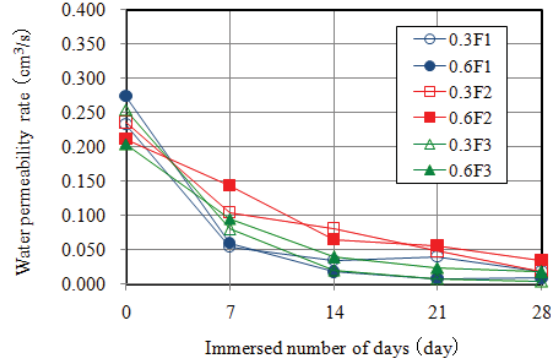


Fig. 6 Permeability test results Initial permeability rate $0.25 \text{ cm}^3/\text{s}$

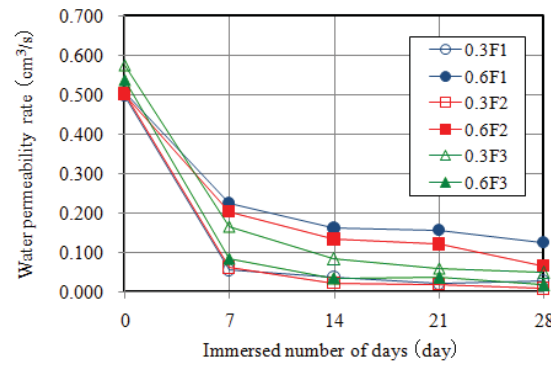


Fig. 7 Permeability test results Initial permeability rate $0.55 \text{ cm}^3/\text{s}$

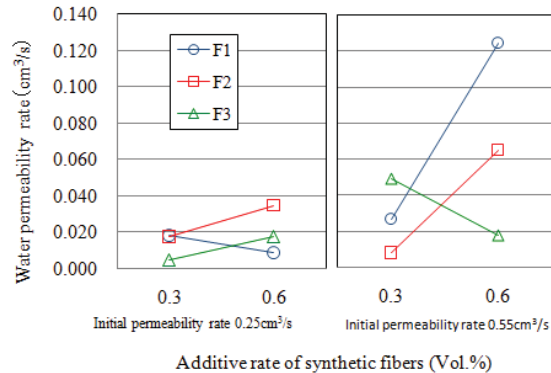


Fig. 8 Relationship of the additive rate of synthetic fibers and permeability rate (dipping 28 days)

C. Microscopy Observation

Figs. 9 and 10 show microscopy photographs of two example mixtures: mixture (0.3F3), which showed the lowest permeability rate, with an initial permeability rate of $0.25 \text{ cm}^3/\text{s}$, which was thought to give high self-healing performance, and mixture (0.6F1), with an initial permeability rate of $0.55 \text{ cm}^3/\text{s}$, which was thought to give low self-healing performance. Fig. 9 shows complete filling of cracks. Fig. 10 does not show complete filling, although the crack width is reduced. Fig. 11 shows a photograph of the surface of mixture (0.3F3), evaluated to have high self-healing performance based

on the extent to which the cracks were filled, with an initial permeability rate of $0.55 \text{ cm}^3/\text{s}$. Despite the surface filling observed, the results of the permeability test (Fig. 11) indicate that the crack was not entirely filled. This difference arises because microscopy examines only surfaces, whereas permeability testing accurately evaluates the extent of self-healing inside the cracks. This suggests that permeability testing is an effective way to quantitatively assess self-healing performance.

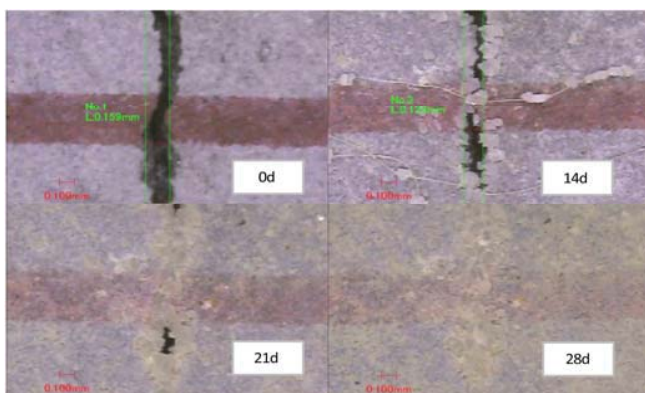


Fig. 9 Self-curing properties of 0.3F3 (0.25)

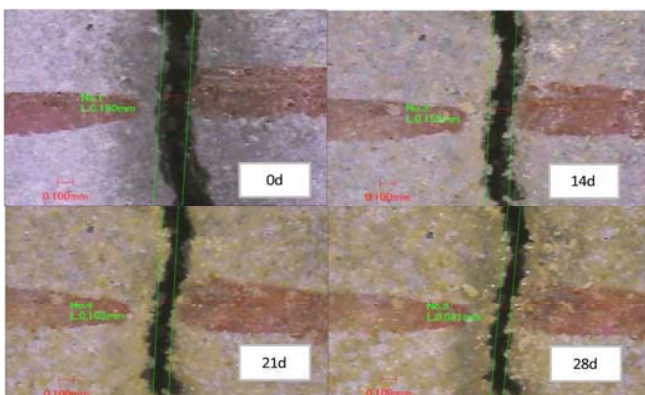


Fig. 10 Self-curing properties of 0.6F1 (0.55)

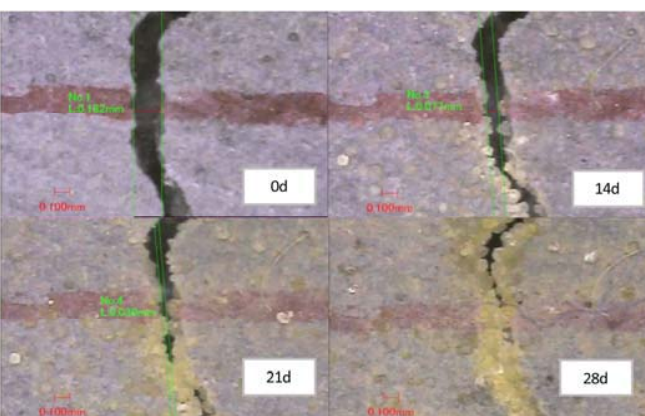


Fig. 11 Self-curing properties of 0.3F3 (0.55)

IV. CONCLUSIONS

The crack self-healing performance of steam cured heavyweight concrete can be summarized as follows:

- 1) Heavyweight concrete manufactured by steam curing at 40°C maximum temperature has good self-healing performance and has performances for demolding strength requirements.
- 2) Heavyweight concrete including synthetic fibers reduces the permeability coefficient on water immersion in cracks and increases self-healing performance.
- 3) There is no difference between various synthetic fibers, such as polypropylene short fiber, nylon short fiber, and vinylon short fiber, on the improvement of self-healing performance. Optimum mixing contents of fibers for improving the self-healing performance were proposed.

REFERENCES

- [1] Kitsutaka Y., Ogawa Y., Yokomuro T., Igawa H. (2014), Evaluation of x-ray shielding performance for concrete box culvert by using x-ray digital image and double layer value analysis method, Proceedings of the Japan Concrete Institute, 36(1), 1990-1995, (in Japanese).
- [2] Sakamoto H. (2016), Shielding of radiation by concrete, Journal of Concrete Technology, 31(6), 63-68, June
- [3] Sindou Y., Ueda T., Watanabe T. (2010), Study on self-healing effect of fly ash concrete, Proceedings of the Japan Concrete Institute, 32(1), 137-142, (in Japanese).
- [4] Kurita T., Hosoda A., Kobayashi K., Matuda Y. (2009), Influence of the nature of curing water on the healing effect of self-healing concrete, 31(1), 247-252, (in Japanese).
- [5] Koide T., Kishi T., Ahn T., (2012), Fundamental research on self-healing concrete using granulated self-healing materials for cracks, and blast furnace slag aggregate, Proceedings of the Japan Concrete Institute, 34(1), 1408-1413, (in Japanese).
- [6] Arai K., Kitsutaka Y., Tamura M. (2004), Study on the degradation restoration performance and evaluation of the concrete using special mixture material, Summaries of technical papers of annual meeting Architectural Institute of Japan, 207-208, (in Japanese).
- [7] Igawa H., Yokomuro T., Kitsutaka Y., Eguchi H. (2015), Reserch on self-healing performance of heavyweight concrete, Cement Science and Concrete Technology, 69(1), 335-340.
- [8] Koda M., Mihashi H., Nishiaki T., Kikuta T., (2011), Experimental study on self-healing capability of FRCC using synthetic fibers, Summaries of technical papers of annual meeting Architectural Institute of Japan, 777-778, (in Japanese)